The Effect of Weight Fraction on the Microstructure and Mechanical Properties of Aluminum–Cast Iron Slag Composites

Lutiyatmi
Mechanical Engineering Department, Universitas Sebelas Maret, Surakarta, Indonesia
yatmiluti@gmail.com

Eko Surojo
Mechanical Engineering Department, Universitas Sebelas Maret, Surakarta, Indonesia
esurojo@ft.uns.ac.id

Nurul Muhayat
Mechanical Engineering Department, Universitas Sebelas Maret, Surakarta, Indonesia
nurulmuhayat@staff.uns.ac.id

Muizuddin Azka
Research Center for Process and Manufacturing Industry Technology, National Research and Innovation Agency (BRIN), Tangerang Selatan, Indonesia
muizuddin.azka@brin.go.id

Triyono
Mechanical Engineering Department, Universitas Sebelas Maret, Surakarta, Indonesia
triyono74@staff.uns.ac.id (corresponding author)

Received: 14 March 2025 | Revised: 29 April 2025 and 20 May 2025 | Accepted: 21 May 2025

 DOI: https://doi.org/10.48084/etasr.10943

ABSTRACT

In the automotive industry, aluminum pistons have a limited lifespan and eventually turn into waste once they are no longer functional. Addressing the challenge of aluminum piston waste requires innovative recycling and utilization strategies. This study explores the potential of combining two waste materials, aluminum piston waste and cast-iron slag, to create Aluminum Matrix Composites (AMCs) with superior mechanical properties. To ensure uniform matrix properties, aluminum pistons from various sources were remelted into ingots before being used for composite fabrication. The AMCs were produced using the stir casting method, with cast-iron slag added as reinforcement at weight fractions of 0%, 1%, 2%, and 3%. The resulting AMCs were assessed for their microstructure, hardness, tensile strength, and corrosion resistance. The findings showed that increasing the slag content improved the particle distribution, refined the grain size, and significantly increased the hardness from 74.33 HV at 0% slag to 427.28 HV at 3% slag. The tensile strength also increased from 105 MPa with 0% slag to 245 MPa with 3% slag, although the elongation decreased from 12.5% to 5.3%. The SEM analysis revealed a transition in fracture morphology from brittle to more ductile characteristics at higher slag fractions, indicating enhanced matrix-reinforcement bonding. Furthermore, the corrosion rate declined from 0.72659 mm/year at 0% slag to 0.20 mm/year at 3% slag.

Keywords-aluminum matrix composites; piston waste; cast iron slag; stir casting; mechanical properties; corrosion rate

I. INTRODUCTION

The growing demand for materials with superior mechanical properties and high performance continues to drive advancements in Metal Matrix Composites (MMCs). Among these, AMCs stand out due to their exceptional strength, hardness, toughness, and excellent resistance to wear and corrosion. These attributes make AMCs highly suitable for

various industries, including automotive, aerospace, defense, marine, and other high-tech sectors [1-4]. AMCs typically consist of an aluminum matrix reinforced with ceramic particles or other elements, such as SiC, Al_2O_3, TiO_2, graphite, as well as industrial and agricultural waste, highlighting their versatility and sustainability potential [5, 6]. Authors in [7] investigated Al–Si alloys fabricated using slag molds and reported a strong correlation between the secondary dendrite arm spacing and improved hardness and strength, indicating the effectiveness of slag in influencing the microstructure and mechanical behavior of the composite. The recycling potential of foundry slags was examined in [8] and their contribution to enhanced performance in casting applications was highlighted. Similarly, authors in [9] evaluated mineral waste slag with varying particle sizes and demonstrated that an optimal particle distribution can significantly improve compressive strength and stability. In [10], the physical and chemical properties of Fe–Cr and blast furnace slags were analyzed, showing their potential as reinforcing agents due to their high silica and ceramic content, which contribute to increased wear resistance and hardness.

Cast-aluminum pistons are extensively used in the automotive sector. However, they have a finite service life and ultimately become waste, contributing to environmental concerns if not properly managed. This growing accumulation of aluminum piston waste necessitates the development of innovative recycling strategies. One sustainable and value-added solution is to repurpose aluminum piston waste as a matrix material for AMCs. Although remelting the pistons into ingots for reuse is possible, this process may alter their original alloy characteristics and mechanical properties [11]. In contrast, direct utilization in AMCs preserves much of the material composition while reducing the processing requirements. In addition, cast-iron slag, an industrial byproduct typically rich in ceramic compounds and silicates, such as SiO_2, offers a cost-effective and sustainable alternative as a reinforcement material [12]. Its natural hardness and abrasive resistance make it particularly suitable for enhancing the wear and mechanical performance of AMCs. This makes them attractive alternatives not only for reducing environmental impact, but also for lowering production costs in AMC fabrication, thereby highlighting the uniqueness and practical relevance of the material selection in this study. To fabricate AMCs, various techniques have been developed, with stir casting using sand molds being one of the most effective and widely employed methods [12]. The properties of AMCs are significantly influenced by the weight fractions of the matrix and reinforcement materials. These fractions govern the uniformity of particle distribution, the interfacial bonding between the matrix and reinforcement, and the overall microstructural homogeneity of the composite [13, 14].

Previous studies have investigated the effects of weight fraction on the properties of AMCs using high-purity reinforcements, such as alumina (Al_2O_3) [13], silicon carbide (SiC) [14], and silicon carbide particles (SiCp) [15]. However, these studies predominantly employed high-purity aluminum and reinforcement materials, overlooking the potential of industrial waste as a raw material. Industrial waste materials often exhibit heterogeneous properties that can introduce variability into recycled composites. This variability underscores the importance of research focused on establishing a database for utilizing industrial waste in AMCs, laying the groundwork for broader adoption and application. This study aims to address these gaps by leveraging two types of waste, aluminum piston waste and cast-iron slag, to develop Al/slag composites with varying weight fractions. The composites were thoroughly evaluated for their physical, mechanical, and corrosion properties to determine their feasibility and potential for industrial applications, contributing to sustainable material innovation.

II. METHODS

A. Materials

The primary material utilized in this study consisted of waste pistons sourced from motorcycles and cars of various brands and models. To achieve material homogeneity and ensure consistency in composition, the pistons were remelted and subjected to thorough Optical Emission Spectroscopy (OES). The results of the chemical composition testing for the remelted pistons are detailed in Table I. The cast-iron slag used in this study was sourced from waste generated by a local foundry industry. It was ground and sieved to a fine powder with a particle size of 200 mesh before being incorporated into the aluminum matrix using the stir casting method. Due to its ceramic and silicate (SiO_2) content, the slag was chosen as a reinforcing material for the AMC. The chemical composition of the slag, analyzed using OES, is shown in Table II, with the primary elements being oxygen, silicon, carbon, manganese, aluminum, and iron.

TABLE I. CHEMICAL COMPOSITION OF THE REMELTED PISTONS

Material	% wt						
	Al	Si	Fe	Cu	Mg	Ni	Zn
Remelted pistons	82.74	12.41	0.529	1.751	0.598	1.080	0.722

TABLE II. CHEMICAL COMPOSITION OF SLAG

Material	% wt					
	O	Si	Al	Mn	Fe	C
Slag	60.88	25.81	3.63	4.12	1.20	4.35

B. Stir Casting Process and Properties

This study investigates the development of AMCs using piston waste as the matrix material and slag as the reinforcement. Slag, a byproduct of the cast-iron casting process, undergoes a refinement process involving crushing, sieving, and selection to obtain particles with an average size of approximately 300 µm. The choice of slag as reinforcement is based on its potential to enhance the mechanical properties of the composite while promoting sustainable waste utilization. The fabrication process begins with melting the piston waste at 670 °C, ensuring complete liquefaction before the gradual addition of slag particles. The slag is introduced incrementally to achieve the predetermined weight fractions of 0%, 1%, 2%, and 3%, allowing controlled dispersion within the aluminum matrix. To ensure uniform particle distribution, the molten aluminum-slag mixture undergoes mechanical stirring using

the stir casting method. This process is carried out for 5 min at a stirring speed of 500 rpm, a parameter optimized to enhance particle homogenization without excessive oxidation or sedimentation. Following the mixing process, the composite melt is poured into greensand molds, which are selected due to their superior moldability and ability to produce smooth surface finishes. Two mold geometries are employed: a plate with dimensions of 400 mm × 140 mm × 4 mm, suitable for mechanical property evaluation, and a cylindrical shape with a diameter of 18 mm and a length of 25 mm, ideal for corrosion and metallographic analysis. The use of greensand molds not only simplifies the casting process, but also ensures a cost-effective and scalable manufacturing approach. The solidified castings undergo a comprehensive evaluation to assess their material characteristics and performance. The analysis includes composition verification, metallographic examination to study the microstructure, corrosion resistance testing, tensile strength measurement, and hardness evaluation. These tests provide insights into the influence of slag reinforcement on the mechanical and structural integrity of the AMC. The overall process of manufacturing the Al/slag composite, including material preparation, casting, and testing, is illustrated in Figures 1 and 2.

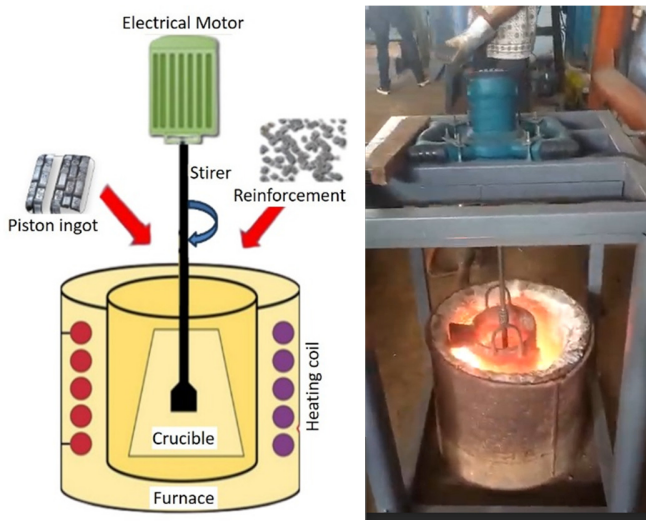

Fig. 1. Stir casting process: (a) schematic and (b) actual process.

C. Aluminum Matrix Composite Characterization

The fabricated Al/slag composites were characterized using a series of tests to evaluate their chemical composition, mechanical properties, corrosion resistance, and microstructure. These tests were conducted using standardized procedures to ensure accuracy and repeatability.

The chemical composition analysis was performed using OES to determine the elemental composition of the material. This test was conducted with a Bruker Q2 ION spectrometer (serial number 214865), manufactured in Germany. OES is a widely used technique that provides precise and rapid analysis of metal alloys, ensuring that the material composition aligns with the intended specifications.

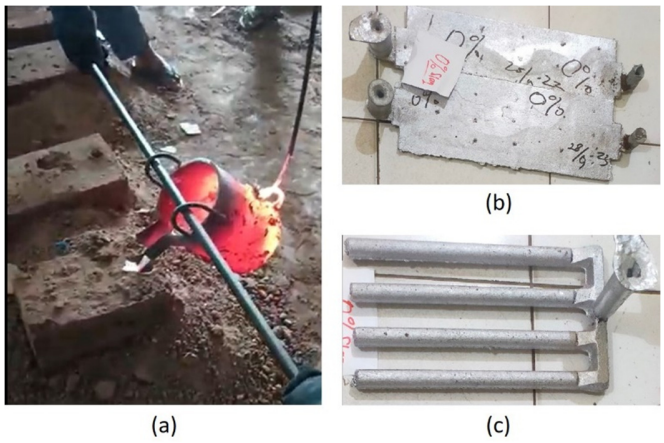

Fig. 2. (a) Pouring process, (b) cast-plate, (c) cast-cylinder.

The Al/slag composite hardness tests were performed using two different methods: Rockwell B and Micro-Vickers. The Rockwell B test, following ASTM E18, utilized a 1/16-inch steel ball indenter to assess the bulk (macroscopic) hardness of the specimen. It was carried out using an AFFRI hardness tester (serial number 251927) from the United Kingdom. On the other hand, the Vickers test, based on ASTM E384, employed a diamond pyramid indenter to evaluate local (microscopic) hardness on the microstructure. These methods assess the resistance of a material to permanent deformation by measuring the size or depth of the indentation left by a standardized indenter under a specific load. Therefore, the presence of permanent deformation is expected and forms the basis for calculating the hardness value. All the measurements were conducted in accordance with the standard, ensuring proper surface preparation, appropriate load application, and adequate specimen thickness. The deformation observed was within the acceptable limits for the respective test standards and did not indicate erroneous hardness readings.

The tensile strength of the material was evaluated according to the JIS Z 2201 standard, and the specimen dimensions are shown in Figure 3. Tensile testing was conducted using a Universal Testing Machine (UTM) manufactured by Hung Ta (serial number 1176) from Taiwan. This test is essential for determining the mechanical properties of the material, including the ultimate tensile strength, yield strength, and elongation, which are the key indicators of the structural performance of the composite.

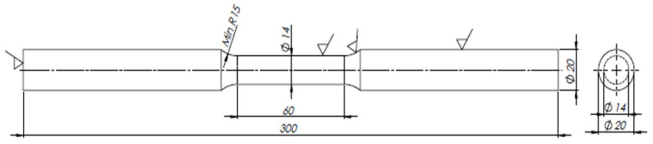

Fig. 3. Specimen dimensions for tensile strength test.

The corrosion resistance of the Al/slag composite was examined following the ASTM G102-89 standard. The test was conducted using a Corrtest CS350M corrosion testing instrument, which enables electrochemical measurements of the material's corrosion rate. The dimensions of the corrosion

test specimens are shown in Figure 4. The corrosion behavior of the Al/slag composites was assessed using potentiodynamic polarization tests conducted in a standard three-electrode electrochemical cell at room temperature. A Saturated Calomel Electrode (SCE) served as the reference electrode, a platinum rod was used as the counter electrode, and the composite sample functioned as the working electrode. The electrolyte used was a 3.5 wt.% NaCl solution, chosen to simulate a marine environment. Before testing, the samples were mechanically polished with 1200-grit sandpaper, then rinsed with distilled water and dried. The Open Circuit Potential (OCP) was monitored for 10 min to ensure stabilization. Polarization measurements were performed by sweeping the potential from −1250 mV to −200 mV at a scan rate of 10 mV/s. The corrosion potential (E_{corr}) and corrosion current density (I_{corr}) were obtained using Tafel extrapolation. The corrosion rate was then calculated using:

$$CR = 0.00327 \times \frac{(I_{corr} \times EW)}{\rho} \quad (1)$$

where CR is the corrosion rate in mm/year (mmpy), I_{corr} is the corrosion current density in μA/cm², ρ is the material density in g/cm³ (measured from the mass and volume of each AMC sample), and EW is the equivalent weight, calculated based on the chemical composition, atomic mass, and valence of each element in the AMC.

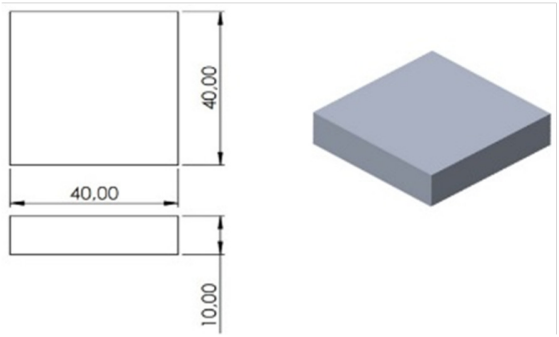

Fig. 4. Dimensions of the specimens used for the corrosion test.

The microstructural analysis of the Al/slag composite was carried out using two different methods: optical microscopy and Scanning Electron Microscopy (SEM). The optical microscopy examination was conducted using a Nikon optical microscope (serial number 661103), which allows for the observation of grain structure and phase distribution. Additionally, a Thermo Scientific SEM was employed to obtain high-resolution images of the composite's surface morphology, revealing finer details, such as particle distribution, porosity, and interfacial bonding between matrix and reinforcement.

III. RESULTS AND DISCUSSION

A. Chemical Composition

The chemical compositions of the Al/slag composites produced by melting aluminum with cast-iron slag at weight fractions of 0%, 1%, 2%, and 3% are detailed in Table III. The data indicate that increasing the slag content leads to a higher percentage of Si, which is expected because of the presence of SiO_2 in cast-iron slag. Additionally, the Fe content rises with increased slag addition, suggesting that the slag contributes to the iron content in the composite. Other elements, such as Cu, Ni, Mg, Cr, and Zn, exhibit fluctuations without a clear trend. The enhancement in the Si content within the AMC is significant, as Si is known to improve the strength and wear resistance of the alloy. Aluminum-silicon alloys, particularly those with silicon content ranging from 6% to 12%, demonstrate optimal mechanical properties, including increased hardness and reduced thermal expansion, making them suitable for applications requiring durability and dimensional stability. Conversely, the observed decrease in Cu and Ni content may positively influence the material's corrosion resistance and weldability. Aluminum-copper alloys, while offering high strength, often face challenges related to corrosion susceptibility and weldability. A reduction in the copper content can mitigate these issues, leading to improved performance in corrosive environments and enhanced joining capabilities.

Based on this analysis, the Al/slag composite with 3% cast-iron slag addition appears superior to the initial aluminum waste composition before AMC fabrication. The increased Si content in this composition provides enhanced mechanical properties, better corrosion resistance, and improved weldability, making it more advantageous compared to the initial AMC material composition.

TABLE III. CHEMICAL COMPOSITION OF AL/SLAG COMPOSITE

No.	Weight fraction	% wt						
		Al	Si	Fe	Cu	Mg	Ni	Zn
1.	Al/slag 0%	83.84	12.17	0.400	1.481	0.933	0.785	0.109
2.	Al/slag 1%	83.21	12.33	0.466	1.392	1.068	1.089	0.176
3.	Al/slag 2%	83.63	12.44	0.445	1.263	0.942	0.940	0.070
4.	Al/slag 3%	83.60	12.81	0.400	1.247	0.810	0.675	0.150

B. Microstructure

The microstructural analysis of the Al/slag composite with varying cast-iron slag weight fractions reveals significant transformations correlating with increased slag content. As depicted in Figure 5a, the base material primarily consisted of the α-Al and eutectic Al-Si phases. With the addition of cast-iron slag, there is a notable increase in the presence of the Al-Si phase, accompanied by a refinement in grain size, as illustrated in Figures 5b–d. This refinement occurs because cast-iron slag contains oxide-based compounds that act as nucleation sites for grain formation. A higher weight fraction of slag provides more nucleation sites, thereby restricting grain growth and resulting in a finer microstructure. This phenomenon is crucial, as finer grains introduce more grain boundaries, which serve as barriers to dislocation movement, enhancing the material's hardness through grain boundary strengthening [16]. Beyond grain refinement, cast-iron slag also contributes to the reinforcement of the aluminum matrix by introducing SiO_2 particles. These particles are dispersed throughout the matrix, impeding dislocation motion and obstructing crack initiation and propagation. This mechanism aligns with particle dispersion strengthening, where the presence of uniformly distributed

second-phase particles enhances the composite's mechanical properties by preventing plastic deformation and increasing resistance to external stresses [15].

The correlation between microstructural evolution and mechanical properties is evident in the hardness measurements of the AMC. As the slag weight fraction increases, the hardness of the material correspondingly improves, highlighting the beneficial impact of cast-iron slag addition. The uniform dispersion of slag particles and the resulting grain refinement contribute significantly to this enhancement. However, excessive slag content may lead to particle agglomeration or porosity, which could compromise the mechanical performance by introducing stress concentration points and reducing the overall toughness [16, 17].

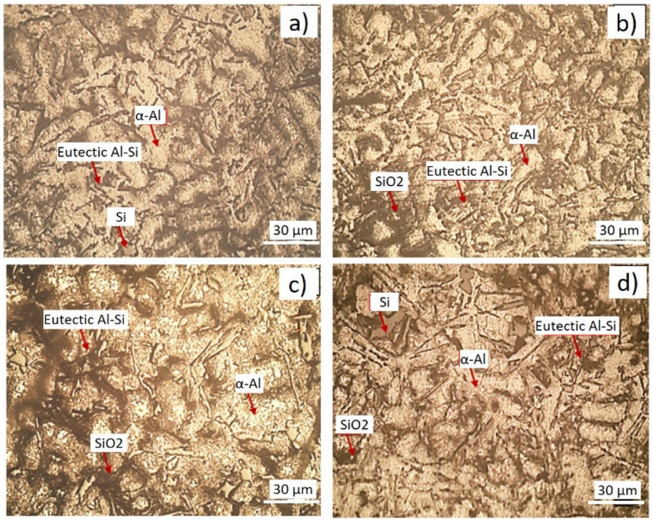

Fig. 5. Microstructure of (a) Al/slag 0%, (b) Al/ slag 1%, (c) Al/ slag 2%, and (d) Al/slag 3%.

C. Hardness

The bulk (macroscopic) hardness test results of the Al/slag composites with varying cast-iron slag content, measured using the Rockwell B scale, are presented in Figure 6. These results demonstrate a clear trend of increasing hardness with higher weight percentages of cast-iron slag. This enhancement in bulk hardness can be attributed to several contributing factors. First, the incorporation of silicon-rich slag particles provides a reinforcing effect by impeding dislocation motion within the aluminum matrix, thus increasing resistance to plastic deformation [13]. Second, the occurrence of dynamic recrystallization during processing promotes grain refinement, which increases the density of grain boundaries. These boundaries act as additional barriers to dislocation motion, thus contributing to improved hardness [14]. Third, the more uniform distribution of slag particles at higher concentrations reduces the localized weak zones within the matrix, leading to a more homogeneous and mechanically resilient composite.

In addition to macroscopic hardness, localized (microscopic) hardness was assessed using the Vickers test, as shown in Figure 7.

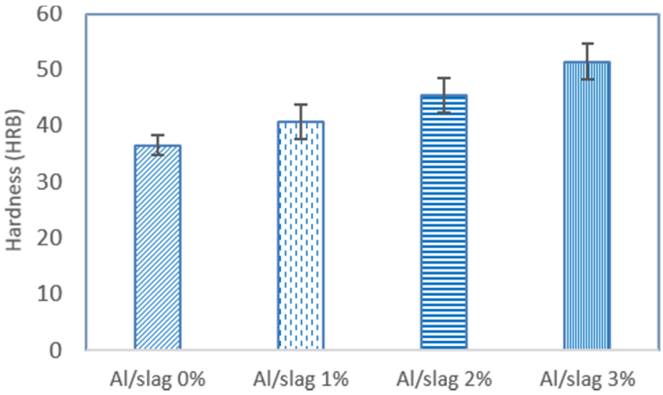

Fig. 6. The Rockwell B hardness of AMCs.

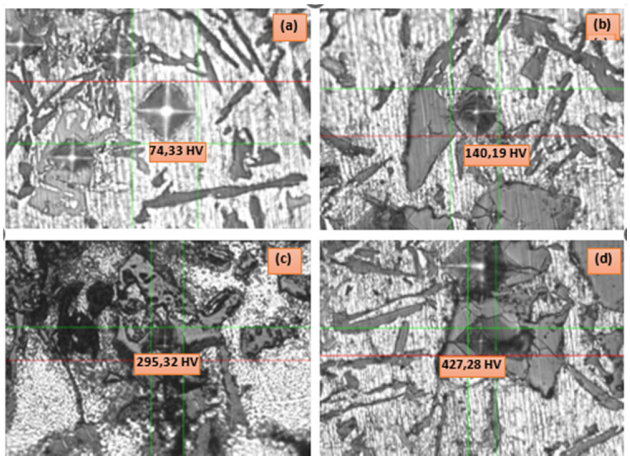

Fig. 7. Indentation of Vickers microhardness test (a) 0%, (b) 1%, (c) 2%, and (d) 3% slag content.

These micro-indentation results provide insight into the evolving microstructural characteristics with varying slag content. Figure 7a presents an indentation with a relatively low hardness value of 74.33 HV, indicative of a soft matrix, likely dominated by pure aluminum with minimal reinforcement. Figure 7b displays a moderate increase in hardness to 140.19 HV, reflecting the initial influence of the dispersed slag particles acting as a strengthening phase. A more pronounced increase is observed in Figures 7c and d, where the hardness values reach 295.32 HV and 427.28 HV, respectively. These values stress the significant contribution of increased slag content to microstructural refinement and effective reinforcement dispersion throughout the matrix. The progressive increase in Vickers hardness demonstrates the positive correlation between slag content and mechanical strengthening. The uniform distribution of slag particles enhances load transfer efficiency and improves the composite's resistance to localized deformation. Nevertheless, potential drawbacks, such as slag particle agglomeration or porosity formation, should be acknowledged, as they may introduce local variations in hardness and compromise the structural integrity in isolated regions. Overall, both Rockwell and Vickers hardness measurements emphasize the critical role of cast-iron slag as a reinforcing agent in AMCs. The improvements in both macroscopic and microscopic hardness

suggest that cast-iron slag incorporation enhances not only the structural integrity, but also the potential applicability of these composites in load-bearing or wear-resistant components.

D. Corrosion Rate

The corrosion test results were obtained through potentiodynamic polarization tests, and Tafel diagrams are presented in Figure 8. From these diagrams, the corrosion current density (I_{corr}) values were determined using Tafel extrapolation. Subsequently, the Equivalent Weight (EW) of each Al/slag composite was calculated based on the chemical composition data presented in Table III, considering the atomic mass and valence number of each element. Using the obtained I_{corr}, the calculated EW, and the experimentally measured density (ρ) of each composite, the corrosion rate (in mm/year) was calculated using (1). The summarized results of these calculations are portrayed in Table IV and are graphically depicted in Figure 9.

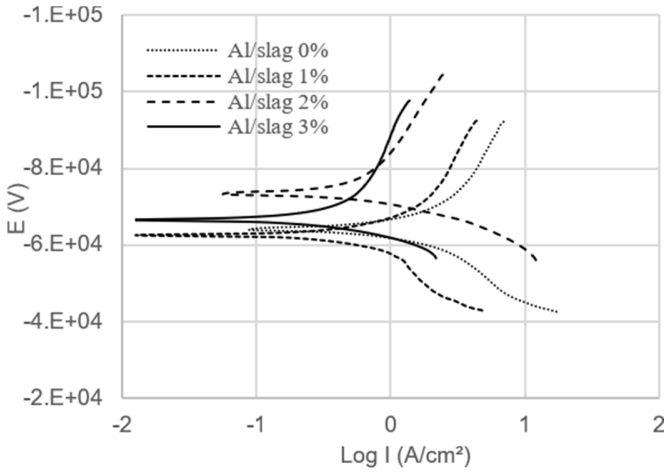

Fig. 8. Tafel diagram of AMCs.

Based on Figure 9, the corrosion test results demonstrate that incorporating cast-iron slag into the Al/slag composite significantly enhanced its corrosion resistance. The lowest corrosion rate was observed in composites containing 2% and 3% slag, with values of approximately 0.204 mm/year, which is a significant reduction compared to the composite without slag (0.727 mm/year). This substantial improvement suggests that cast-iron slag plays a crucial role in mitigating corrosion, potentially by forming a more stable and protective surface layer that limits material degradation. However, it is important to acknowledge that ceramic-based composites, such as Al/slag, typically present challenges, including poor wettability between the matrix and reinforcement and the tendency for particle agglomeration, both of which can adversely affect the composite's toughness and ductility [18].

TABLE IV. CORROSION RATE CALCULATION

AMC	Density (g/cm^3)	EW	I_{corr} (µA/cm^2)	CR (mmpy)
Al/slag 0%	2.7	8.928	67.2	0.727
Al/slag 1%	2.8	8.947	62.0	0.648
Al/slag 2%	2.85	8.914	19.9	0.204
Al/slag 3%	2.95	8.890	24.5	0.241

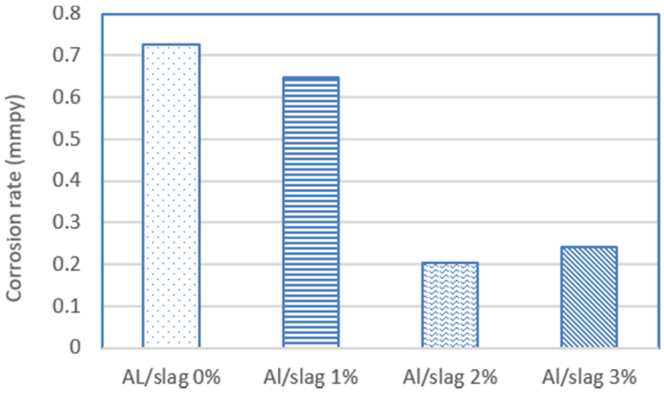

Fig. 9. Corrosion rate of AMCs.

Despite these limitations, the corrosion test results emphasize the strong potential of Al/slag composites as materials with enhanced corrosion resistance. Optimizing the slag content and dispersion techniques could further improve their performance, making them viable for applications in corrosive environments. The corrosion test results for the Al/slag composite samples highlight the effectiveness of slag addition in reducing corrosion susceptibility.

E. Tensile Strength

The tensile test results demonstrate the effect of increasing cast-iron slag content on both the tensile strength and elongation of the Al/slag composite, as illustrated in the stress-strain curves in Figure 10. From these curves, the quantitative values of tensile strength and elongation were calculated and are presented in Figure 11. The data confirmed that the addition of slag effectively enhanced the strength of the material by impeding plastic deformation. This improvement is primarily attributed to grain boundary strengthening, where the dispersed slag particles serve as obstacles to dislocation motion, resulting in grain refinement and improved mechanical properties. However, as the slag content increased, a slight decrease in elongation was observed. This minor reduction in ductility is caused by the presence of rigid slag particles that locally hinder plastic flow, though the composite overall still maintains a reasonable degree of formability.

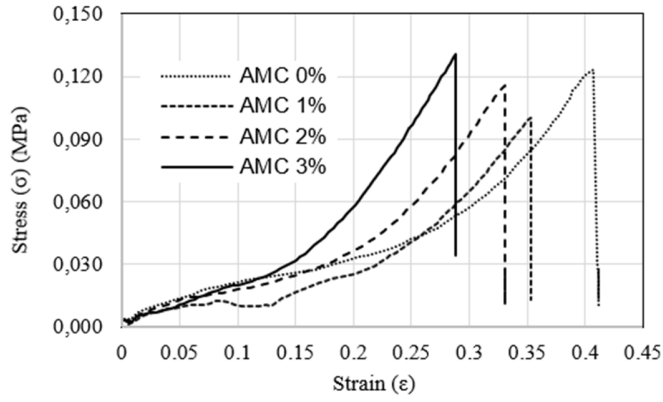

Fig. 10. Stress-strain diagram of AMCs.

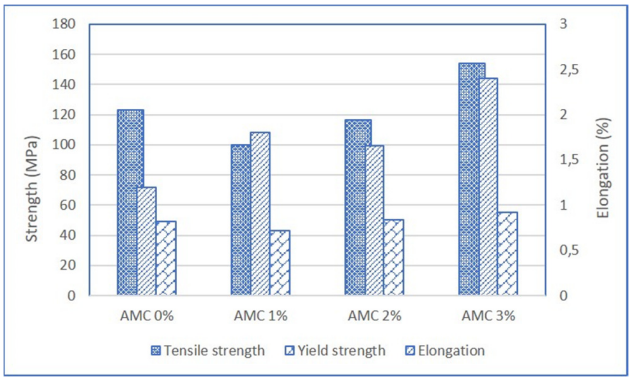

Fig. 11. Tensile strength of Al/slag composites.

However, while a higher slag content enhances the tensile strength, it adversely affects the ductility, as evidenced by a reduction in the elongation. This suggests a trade-off between strength and toughness, where an excessive slag content may lead to embrittlement [19]. Additionally, inhomogeneous slag distribution, particularly particle agglomeration, can introduce defect sites that compromise the material integrity. Therefore, ensuring the uniform dispersion of slag particles is crucial for achieving optimal mechanical performance. The fracture characteristics of the Al/slag composite offer further insight into its failure mechanisms. Figure 12 presents macro-fracture analyses of the tensile test specimens with 0%, 1%, 2%, and 3% slag content, revealing that increasing the slag content alters the fracture morphology. The observed fracture patterns indicate variations in hardness, brittleness, and ductility, reflecting changes in the composite's deformation behavior.

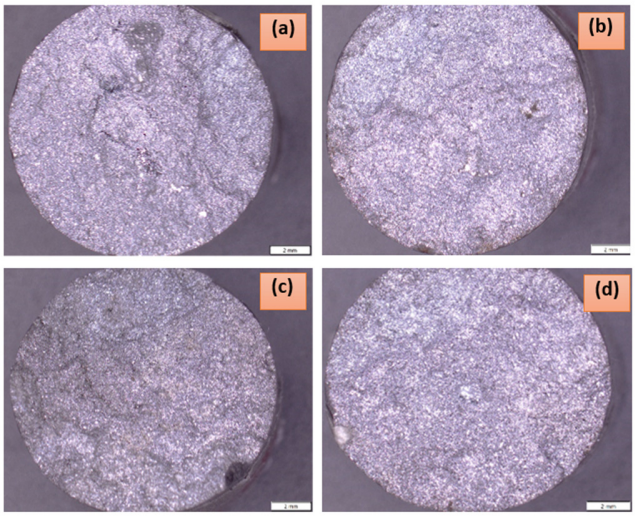

Fig. 12. Surface fracture of tensile testing for Al/slag composite (a) 0%, (b) 1%, (c) 2%, and (d) 3%.

To gain a more detailed understanding of slag distribution, morphology, and matrix-reinforcement interaction, SEM analysis was performed. Figure 13 illustrates the microstructural evolution across different slag concentrations. As shown in Figure 13a (0–1% slag), brittle cracks dominated the fracture surface, indicating low ductility. In Figure 13b (2% slag addition), the presence of brittle fractures decreased, suggesting improved load transfer between the matrix and reinforcement. As shown in Figure 13c (3% slag addition), the fracture surface exhibited ductile failure, indicating an increased energy absorption before fracture.

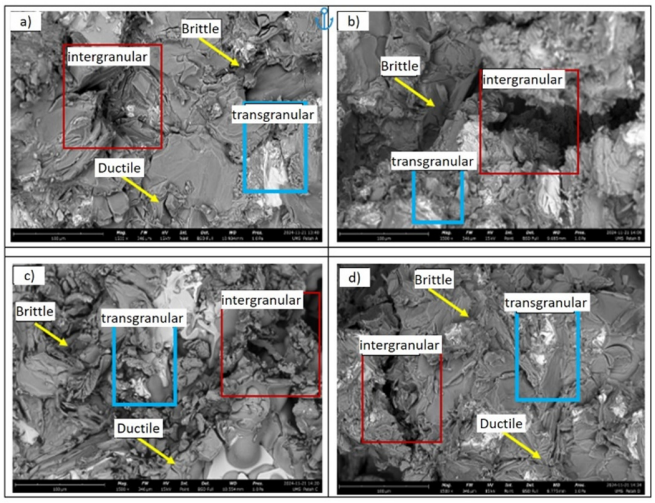

Fig. 13. SEM images of fractured surfaces at (a) 0%, (b) 1%, (c) 2%, and (d) 3% slag content.

These results confirm that slag addition significantly influences the fracture behavior, where an optimal slag fraction enhances ductility and toughness by promoting a better matrix-reinforcement bond. This highlights the potential of Al/slag composites as structural materials with improved mechanical performance when slag distribution is carefully controlled.

IV. CONCLUSIONS

This study demonstrates the feasibility of utilizing aluminum piston waste as a matrix and cast-iron slag as reinforcement in the fabrication of Aluminum Matrix Composites (AMCs) through stir casting. The novelty of this study lies in the unique combination of two different industrial waste materials, discarded aluminum pistons and cast-iron slag, as primary constituents in AMC fabrication, which has not been extensively reported in the literature. While earlier studies often utilized synthetic reinforcements, such as SiC or Al_2O_3 or were focused solely on a single type of industrial waste, this work proposes a dual-waste approach that not only yields favorable material properties, but also promotes sustainability. The chemical composition analysis reveals that increasing the weight fraction of slag enhances the silicon content, which is known to improve the strength, wear resistance, and dimensional stability of aluminum alloys. Moreover, the microstructural analysis confirms that the presence of slag leads to grain refinement due to its role as a nucleation agent, contributing to a more homogeneous and compact structure. Compared to similar works, the results show competitive or improved performance. For example, previous studies using fly ash or red mud as reinforcement typically reported non-uniform dispersion and limited grain refinement. In contrast,

the use of cast-iron slag in this study resulted in finer grains and more homogeneous structures owing to better wettability and nucleation behavior. Additionally, the 3% slag-reinforced AMC developed in this study exhibited superior chemical and microstructural characteristics compared to conventional slag-free or high-percentage waste composites.

ACKNOWLEDGMENT

The authors gratefully acknowledge the financial support provided by Universitas Sebelas Maret, Surakarta, Indonesia, through the Penelitian Disertasi Doktor grant under contract number 1076.1/UN27.22/PT.01.03/2024.

REFERENCES

[1] C. Saravanan, K. Subramanian, V. A. Krishnan, and S. R. Narayanan, "Effect of Particulate Reinforced Aluminium Metal Matrix Composite," *Mechanics and Mechanical Engineering*, vol. 19, no. 1, pp. 23–30, 2015.

[2] J. Liu *et al.*, "Enhancement of fiber–matrix adhesion in carbon fiber reinforced Al-matrix composites with an optimized electroless plating process," *Composites Part A: Applied Science and Manufacturing*, vol. 142, Mar. 2021, Art. no. 106258, https://doi.org/10.1016/j.compositesa.2020.106258.

[3] N. Ashrafi, A. H. M. Ariff, M. Sarraf, S. Sulaiman, and T. S. Hong, "Microstructural, thermal, electrical, and magnetic properties of optimized Fe_3O_4–SiC hybrid nano filler reinforced aluminium matrix composite," *Materials Chemistry and Physics*, vol. 258, Jan. 2021, Art. no. 123895, https://doi.org/10.1016/j.matchemphys.2020.123895.

[4] B. Park, D. Lee, I. Jo, S. B. Lee, S. K. Lee, and S. Cho, "Automated quantification of reinforcement dispersion in B_4C/Al metal matrix composites," *Composites Part B: Engineering*, vol. 181, Jan. 2020, Art. no. 107584, https://doi.org/10.1016/j.compositesb.2019.107584.

[5] A. Manna, H. S. Bains, and P. B. Mahapatra, "Experimental study on fabrication of Al—Al_2O_3/Grp metal matrix composites," *Journal of Composite Materials*, vol. 45, no. 19, pp. 2003–2010, Sep. 2011, https://doi.org/10.1177/0021998310394691.

[6] U. Aybarc, D. Dispinar, and M. O. Seydibeyoglu, "Aluminum Metal Matrix Composites with SiC, Al_2O_3 and Graphene – Review," *Archives of Foundry Engineering*, vol. 18, no. 2, pp. 5–10, May 2018, https://doi.org/10.24425/122493.

[7] R. K. Yajjala, N. M. Inampudi, and B. R. Jinugu, "Correlation between SDAS and mechanical properties of Al–Si alloy made in Sand and Slag moulds," *Journal of Materials Research and Technology*, vol. 9, no. 3, pp. 6257–6267, May 2020, https://doi.org/10.1016/j.jmrt.2020.02.066.

[8] A. Pribulová, P. Futáš, M. Bartošová, and J. Petrík, "Utilization of Slags from Foundry Process," *Journal of Casting & Materials Engineering*, vol. 1, no. 4, pp. 103–103, 2017, https://doi.org/10.7494/jcme.2017.1.4.103.

[9] M. Chen, P. Wen, C. Wang, Z. Chai, and Z. Gao, "Evaluation of particle size distribution and mechanical properties of mineral waste slag as filling material," *Construction and Building Materials*, vol. 253, Aug. 2020, Art. no. 119183, https://doi.org/10.1016/j.conbuildmat.2020.119183.

[10] I. Narasimha Murthy and J. Babu Rao, "Investigations on Physical and Chemical Properties of High Silica Sand, Fe-Cr Slag and Blast Furnace Slag for Foundry Applications," *Procedia Environmental Sciences*, vol. 35, pp. 583–596, Jan. 2016, https://doi.org/10.1016/j.proenv.2016.07.045.

[11] S. Thirumalvalavan and N. Senthilkumar, "Evaluation of mechanical properties of aluminium alloy (LM25) reinforced with fused silica metal matrix composite," *Indian Journal of Engineering and Materials Sciences*, vol. 26, no. 1, pp. 59–66, 2019.

[12] A. Arifin, Gunawan, I. Yani, M. Yanis, and R. Pradifta, "Optimization of Stir Casting Method of Aluminum Matrix Composite (AMC) for the Hardness Properties by Using Taguchi Method," *Jurnal Kejuruteraan*, vol. 29, no. 1, pp. 35–39, 2017, https://doi.org/10.17576/jkukm-2017-29(1)-04.

[13] M. Kök, "Abrasive wear of Al_2O_3 particle reinforced 2024 aluminium alloy composites fabricated by vortex method," *Composites Part A: Applied Science and Manufacturing*, vol. 37, no. 3, pp. 457–464, Mar. 2006, https://doi.org/10.1016/j.compositesa.2005.05.038.

[14] S. Tzamtzis, N. S. Barekar, N. Hari Babu, J. Patel, B. K. Dhindaw, and Z. Fan, "Processing of advanced Al/SiC particulate metal matrix composites under intensive shearing – A novel Rheo-process," *Composites Part A: Applied Science and Manufacturing*, vol. 40, no. 2, pp. 144–151, Feb. 2009, https://doi.org/10.1016/j.compositesa.2008.10.017.

[15] J. Jiang, G. Chen, and Y. Wang, "Compression Mechanical Behaviour of 7075 Aluminium Matrix Composite Reinforced with Nano-sized SiC Particles in Semisolid State," *Journal of Materials Science & Technology*, vol. 32, no. 11, pp. 1197–1203, Nov. 2016, https://doi.org/10.1016/j.jmst.2016.01.015.

[16] S. A. Kareem *et al.*, "Aluminium matrix composites reinforced with high entropy alloys: A comprehensive review on interfacial reactions, mechanical, corrosion, and tribological characteristics," *Journal of Materials Research and Technology*, vol. 30, pp. 8161–8186, May 2024, https://doi.org/10.1016/j.jmrt.2024.05.153.

[17] K. Adiga, M. A. Herbert, S. S. Rao, and A. Shettigar, "Applications of reinforcement particles in the fabrication of Aluminium Metal Matrix Composites by Friction Stir Processing - A Review," *Manufacturing Review*, vol. 9, 2022, Art. no. 26, https://doi.org/10.1051/mfreview/2022025.

[18] A. S. Alghamdi, M. Ramadan, K. S. A. Halim, and N. Fathy, "Microscopical Characterization of Cast Hypereutectic Al-Si Alloys Reinforced with Graphene Nanosheets," *Engineering, Technology & Applied Science Research*, vol. 8, no. 1, pp. 2514–2519, Feb. 2018, https://doi.org/10.48084/etasr.1795.

[19] A.-G. Schiopu, B. M. Girish, B. M. Satish, and S. Shubha, "Wear and Hardness Characterisation of Hot Forged Tungsten Carbide reinforced Aluminium 6061 Composite Materials," *Engineering, Technology & Applied Science Research*, vol. 14, no. 1, pp. 12688–12693, Feb. 2024, https://doi.org/10.48084/etasr.6659.